

**Photoinduced oxidation of an indole derivative: 2-(1'H-indol-2'-yl)-[1,5]naphthyridine**

Journal:	<i>Photochemical & Photobiological Sciences</i>
Manuscript ID	PP-ART-12-2018-000587.R1
Article Type:	Paper
Date Submitted by the Author:	22-Feb-2019
Complete List of Authors:	Golec, Barbara; Institute of Physical Chemistry, Nawara, Krzysztof; Faculty of Mathematics and Natural Sciences, College of Science, Cardinal Stefan Wyszyński University Thummel, Randolph; University of Houston, Chemistry Waluk, Jacek; Polish Academy of Sciences, Institute of Physical Chemistry

Photoinduced oxidation of an indole derivative: 2-(1'*H*-indol-2'-yl)-[1,5]naphthyridine

Barbara Golec,^{*a} Krzysztof Nawara,^b Randolph P. Thummel,^c Jacek Waluk^{*a,b}

^a *Institute of Physical Chemistry, Polish Academy of Sciences, Kasprzaka 44/52, 01-224 Warsaw, Poland*

^b *Faculty of Mathematics and Science, Cardinal Stefan Wyszyński University, Dewajtis 5, 01-815 Warsaw, Poland*

^c *Department of Chemistry, University of Houston, Houston, TX, 77204-5003, USA*

* Corresponding authors:

Prof. Jacek Waluk, e-mail: waluk@ichf.edu.pl, Fax: + 48 (22) 3433333

Dr. Barbara Golec, e-mail: bgolec@ichf.edu.pl, Fax: + 48 (22) 3433333.

Dedicated to the memory of Prof. Ugo Mazzucato

Abstract

UV-induced oxidation of 2-(1'*H*-indol-2'-yl)-[1,5]naphthyridine acetonitrile solution in the presence of air leads to formation of 2-(1,5-naphthyridin-2-yl)-4*H*-3,1-benzoxazin-4-one as a major product and *N*-(2-formylphenyl)-1,5-naphthyridine-2-carboxamide as a minor one. The probable reaction mechanisms are different for the two photoproducts and may involve both, the reaction with singlet oxygen generated by the excited substrate or the reaction of the excited substrate with ground state oxygen molecule. Electronic absorption and IR spectra indicate that both photoproducts are formed as mixtures of *syn* and *anti* rotameric forms. The obtained results indicate an efficient and easy method of synthesis of molecules with benzoxazinone structure.

Keywords: benzoxazinones, indole derivatives, heterocycles, photooxidation, UV-A radiation

Introduction

Oxidation of indole and its derivatives has been extensively studied,¹⁻²⁵ because this reaction leads to formation of a variety of products which are of biological as well as synthetic relevance. Important products of indole oxidation include oxindole, isatin, indoxyl, and the oxindole dimers indigo and indirubin.¹ Oxidation of tryptophan, (3-substitued indole derivative) can lead to formation of myriad of products, including hydroxytryptophan, N-formylkynurenine, and kynurenine, depending on the reaction conditions and the oxidizing agent used.³⁻⁶ 2-substitued indole derivatives can be converted to corresponding 2-oxindoles.⁹ Oxidation of 2-arylindoles was reported to produce N-benzoyl anthranilic acid and 2-arylbenzoxazinone derivatives,^{7,8,10} which are important versatile building blocks in organic synthesis and medical chemistry. 4H-3,1-benzoxazin-4-ones are biologically active, for example as inhibitors of serine proteases,^{26,27} as well as inactivators of human leukocyte elastase.²⁸⁻³⁰ Benzoxazinone derivatives reveal a variety of biological effects, such as antifungal, antiviral and antibacterial, antimalarial, antipyretic, anticancer, and anti-HIV activities.^{26,29,31-35}

Previous studies have proved that the indole moiety and its derivatives can be bio-oxidized by various oxygenases, e.g., the bacterial oxygenases¹¹⁻¹³ or the human cytochrome P450 enzyme.¹⁴⁻¹⁶ Various chemical oxidizing agents, such as the oxone (peroxomonosulphate),¹⁷ I₂/TBHP,¹⁸ or HOBr (hypobromous acid)¹⁹ can be used for oxidation. It has also been reported that the oxidation of indole and its derivatives can be induced through photosensitized processes using UV-A (320-400 nm) and visible radiation in the presence of photosensitizers, such as pterins,^{20,21} flavins,^{22,23} or porphyrins.²⁴

4H-3,1-benzoxazin-4-ones are formed from corresponding 2-arylindoles when oxone is used as oxidation agent.⁷ Yamashita and Iida developed a method for the transformation of indoles to benzoxazinones by utilizing a copper catalyst and molecular oxygen as the oxidant.⁸ Garg and Bhakuni reported that 2-phenylbenzoxazinone can be also formed as a result of photooxidation of 2-phenylindole in methanol when Rose Bengal is used as a singlet oxygen sensitizer.²⁵

In this work we show that 2-substitued benzoxazinone structure can be formed upon 365 nm irradiation of a 2-substitued indole derivative, 2-(1'H-indol-2'-yl)-[1,5]naphthyridine (**1**, Scheme 1) in acetonitrile at ambient temperature in the presence of air. In a previous paper,³⁶ we analyzed the photostability of **1** in different – protic and aprotic - solvents, demonstrating that the photodegradation yield can be strongly reduced upon forming intermolecular hydrogen

bonds with alcohols or water. However, the structure of the photoproduct(s) was not determined. Therefore, it was the main objective of the present work. The second goal originated from the finding that **1** exists in solution as a mixture of *syn* and *anti* rotameric forms. Since the photophysical properties of these two species may be different,^{36,37} we wanted to check whether both rotamers undergo phototransformation, and, if so, whether the rates and structures of the photoproducts are similar. Such issues have been discussed in the pioneering works of professor Mazzucato.³⁸

The experimental results, combined with simulations of electronic and IR spectra reveal a rich photochemistry of **1**. Two photoproducts have been observed, each present in two rotameric forms. The major product was identified as 2-(1,5-naphthyridin-2-yl)-4H-3,1-benzoxazin-4-one (**2**). Another photoproduct, obtained with a smaller yield is N-(2-formylphenyl)-1,5-naphthyridine-2-carboxamide (**3**). Generation of **3** is also observed when singlet oxygen is produced using external photosensitizer. Under these conditions, only small amounts of **2** are detected.

Schemes 1-2

Experimental Section

Materials:

2-(1'H-indol-2'-yl)-[1,5]naphthyridine (**1**): The previously reported reaction of 2-acetyl-1,5-naphthyridine with phenyl hydrazine provided the corresponding phenyl hydrazone.^{39,40} Subsequent treatment of this hydrazone with polyphosphoric acid under Fischer indolization conditions gave **1**.

2,3,7,8,12,13,17,18-Octaethyl-21H,23H-porphine palladium(II) (**PdOEP**): The **PdOEP** have been obtained according to the procedure described elsewhere,⁴¹ followed by purification and chromatography separation.

Solvents: Acetonitrile and water (LCMS grade, Merck).

Irradiation conditions:

- A. 365 nm irradiation of **1** in acetonitrile

Light source: High power (270 mW) 365 nm single chip LED diode (Roithner Laser Technik, H2A1-H365-r4). The light intensity was determined by potassium ferrioxalate actinometry as 3.2×10^{16} quanta/s.

Normal sample: Acetonitrile solution of **1** with molar concentration of about 4.0×10^{-5} mol dm⁻³ was irradiated at room temperature in a quartz cuvette in the presence of air. During irradiation, the solution was gently mixed with a magnetic stirrer.

Deaerated sample: The air was removed from the normal sample of **1** in acetonitrile using a freeze-pump-thaw technique (five cycles) down to 10^{-5} Torr.

B. 543 nm irradiation of mixture of **1** and **PdOEP** in acetonitrile

Light source: The sample was irradiated for 130 h at 543 nm (bandpass 10 nm) in the FS5 spectrofluorometer (Edinburgh Instruments) equipped with 150W Xenon-arc lamp.

Sample: Irradiation of mixture of **1** and **PdOEP** was carried out at room temperature in a quartz cuvette using the solution with molar concentration of about 4.8×10^{-5} mol dm⁻³ (**1**) and 2.6×10^{-6} mol dm⁻³ (**PdOEP**) in the presence of air.

Electronic absorption spectra:

Shimadzu UV 2700 spectrophotometer was used to obtain the electronic absorption spectra.

LC-MS studies:

Sample preparation: After certain time of irradiation (0, 1, 2, 3 h for samples of **1** in acetonitrile or 0, 14, 41, and 130 h for samples containing **1** and **PdOEP** in acetonitrile) the irradiated sample solution was transferred into UPLC vials, diluted 10 times with the solvent, and injected into the LC-MS system for the determination of the masses and concentrations of the parent compound and the photoproducts.

The LC-MS system: Reversed-phase high-performance liquid chromatography electrospray ionization mass spectrometry analysis was performed using a Shimadzu Nexara X2 LC/MS/MS 8050 system. Chromatographic separation was achieved with a 00D-4424-B0 Synergi™ 4 μm Fusion-RP 80 Å, LC column 100 × 2 mm (Phenomenex).

The ESI-MS settings were as follows: capillary voltage 4000 V (positive mode) and 3000 V (negative mode), nebulizing gas flow 3.0 L/min, and drying gas flow 5 L/min at 300 °C. The mobile phase was composed of acetonitrile (90 %) and water (10 %). The flow rate was 0.8 mL/min with an isocratic elution. The injection volume was 0.2 μL for **1** in acetonitrile and 0.9 μL for the sample containing **1** and **PdOEP**. The column temperature was set at 40 °C.

The mass-to-charge ratio (m/z) scan range was from 80 to 1000. The concentration of ions assigned to the substrate and to the photoproducts was determined by using selected ion

monitoring (SIM) procedure. The peak areas for individual ion chromatograms were integrated. The LC-MS data were processed using LabSolutions software (Shimadzu).

Infrared studies: The infrared spectra of the substrate and photoproducts were obtained using a Fourier-Transform Infrared (FTIR) spectrometer (Thermo Scientific, Nicolet iS10) with Smart OMNI-Transmission accessory or a Nicolet Continuum FT-IR Microscope with MCT-B detector. The spectra were analyzed using Omnic 9 software. Before irradiation, samples of **1** were mixed with KBr and measured in transmission mode. Samples of **1** in acetonitrile with molar concentration of about $1.8 \times 10^{-4} \text{ mol dm}^{-3}$ after 6.5 h of 365 nm irradiation were placed on top of an aluminum mirror and then, after solvent evaporation, the spectra were recorded using the microscope (co-addition of 256 scans at 4 cm^{-1} resolution over the frequency region of $4000\text{--}450 \text{ cm}^{-1}$). The spectra were ratioed against a background air spectrum.

Computations: Ground state geometries, electronic transition energies, and excited-state geometries were calculated using the density functional theory (DFT) or time-dependent DFT (TDDFT) method with B3LYP functional and 6-31+G(d,p) basis set.^{42,43} All the calculations were performed using the Gaussian 09 suites of programs.⁴⁴

Results and discussion

Solutions of 2-(1'H-indol-2'-yl)-[1,5]naphthyridine in acetonitrile were irradiated at 365 nm using the LED diode. When a sample was irradiated in a presence of air, the degradation of **1** was observed. The photodegradation quantum yield was established as $1.8 \times 10^{-4} (\pm 10\%)$.³⁶ No changes were observed for samples kept in the dark. In the deaerated sample the photodegradation did not occur under our experimental conditions. This suggests photooxygenation as a process that takes place as a result of UV irradiation. Schemes 1 and 2 show the structures of the most probable products of oxidation of **1**, taking into account the products which have been observed before for other substituted indole derivatives.^{1,3–10,26} To establish the nature of the photoproducts we used liquid chromatography tandem-mass spectrometry, electronic absorption, and infrared spectroscopy.

The results of the experimental studies were supported by the results of DFT calculations which allowed us to predict the structures and spectroscopic properties of the photoproducts.

Figure 1 and Figure S1 in Supporting Information show the LC-MS spectra obtained for **1** before and after of 3 h of 365 nm irradiation. The data demonstrate that, as a result of irradiation, the amount of the protonated ions of the substrate ($m/z = 246$) decreases and new products are formed, represented by ions with masses 276 and 278, with the relative ratio of about 4:1, respectively. This ratio does not change for different irradiation times, which indicates that both photoproducts are formed in parallel. The chromatograms of the positive molecular ions $[M + H]^+$ with m/z equal to 246, 276, and 278 determined for acetonitrile solution of **1** before and after 1, 2, and 3 h of 365 nm irradiation are given in Figure S2 and Table S1 in the Supporting Information.

Figure 1

The protonated molecular ion with m/z equal to 276 can be assigned to 2-(1,5-naphthyridin-2-yl)-4H-3,1-benzoxazin-4-one (**2**, Scheme 1), and the mass of 278 to N-(2-formylphenyl)-1,5-naphthyridine-2-carboxamide (**3**, Scheme 1). The yields of the photoproducts, derived from the photodestruction quantum yield and the relative contributions of products **2** and **3** obtained from the LC-MS data have been established as 1.44×10^{-4} and 3.6×10^{-5} ($\pm 10\%$) for molecules **2** and **3**, respectively.

Trace amounts of an $[M + H]^+$ ion with m/z equal to 260 observed in Figure 1, which can be assigned to 2-(1,5-naphthyridin-2-yl)-3H-indol-3-one (**4**, Scheme 2) did not increase under irradiation, suggesting that this type of product is not formed under our experimental conditions.

In the LC-MS spectra of **1** after irradiation (Figure S1b in Supporting Information) we observed a signal of a negative ion with the mass of 292, which can be attributed to 2-[(1,5-

naphthyridine-2-carbonyl)amino]benzoic acid (**5**, Scheme 2), at the level of background noise. According to previous data this molecule can be formed as a result of hydrolysis of **2**.⁸ To verify this hypothesis, some amounts of water (about 10% of sample volume) were added to the sample obtained as a result of UV irradiation of **1**. Then, the signal with the mass 292 clearly appeared in the spectrum.

The results of DFT calculations indicate that molecules **1** and **2** can exist in two stable conformations, *syn* and *anti*. For molecule **3** twelve rotameric forms have been predicted (Figure S3, Supporting Information). Figure 2 shows the two most stable structures of **1-3** and their relative zero-point corrected energies. The energy gap between the *syn*- and *anti*- forms of the substrate amounts to 4.5 kcal mol⁻¹,³⁶ and for **2** (**2a** and **2b**, respectively) it is predicted as 1.3 kcal mol⁻¹. For molecule **3** the structure **3b** is less stable by 5.4 kcal mol⁻¹ than **3a**.

Figure 2

The left panel of Figure 3 shows the comparison of the experimental electronic absorption spectra obtained for **1** in acetonitrile before irradiation with the TDDFT-simulated spectra of isomers **1a** and **1b**. In the right panel the experimental spectrum recorded for the irradiated sample is compared with the absorption predicted for molecules **2a**, **2b**, **3a**, and **3b**. The calculated energies and oscillator strengths of the lowest twelve electronic transitions of these structures are listed in Table S2 in Supporting Information.

Figure 3

The low energy absorption band of **1** observed in the spectrum before irradiation corresponds more likely to the *syn* isomer (**1a**). However, according to our previous fluorescence decay studies in acetonitrile, the *anti*-isomer is also present. The relative contributions have been estimated from the values of amplitudes in the fluorescence decay curves as 75% and 25 % for *syn*- and *anti*-structures, respectively.³⁶

According to the simulations, the experimental absorption recorded after irradiation can originate from all the structures **2a**, **2b**, **3a**, and **3b**, as shown in Figure 3. Some trace amounts of **1** can also be still present in the solution. As already mentioned, the LC-MS gave the relative ratio of 4:1 of the products **2** and **3**. Inspection of the absorption spectrum obtained after irradiation strongly suggests the presence of several species, as at least six bands can be distinguished in the region between 26000-35000 cm^{-1} . Based on the results of calculation, one can tentatively assign the low energy shoulder located at around 28500 cm^{-1} to compound **3**, whereas the maximum at ca. 29500 cm^{-1} to structure **2**.

The experimental FTIR spectra of the non-irradiated sample of **1** compared with the simulated infrared spectra of **1a** and **1b** rotameric structures of this compound are presented in Figure 4. The obtained data suggest that experimental spectrum contains the vibrational lines of both rotamers. In particular, it would be hard to interpret the rich spectral pattern in the region of 1200-1400 cm^{-1} assuming the presence of only one species. Estimation of the relative contributions of **1a** and **1b** is not easy, since most of the vibrational frequencies are predicted to be similar in both forms. However, one can make such attempt, based on the shape of the bands corresponding to two strong transitions observed at 1492 and 1541 cm^{-1} . They both display a shoulder at the low frequency side. The calculations predict a shift to lower energy in **1b** for both transitions (see Figure 4). Thus, the shape of the two bands can be explained by assuming that in both cases the maximum corresponds to **1a**, whereas the shoulder, to **1b**, present in smaller amount. Such conclusion agrees with the 3:1 ratio estimated from fluorescence (*vide supra*); it can also be reinforced by a very good agreement between the experimental and simulated vibrational transition energies.

Figure 4

The infrared spectrum recorded for **1** after 365 nm irradiation is presented in Figure 5, along with the DFT simulated IR spectra for structures of products **2a**, **2b**, **3a**, and **3b**. The

obtained data indicate that the experimental absorption cannot be reproduced by any of the single components. We also cannot exclude the existence of small amounts of the substrate which also can interfere with the lines of products. All the structures **2a**, **2b**, **3a**, and **3b** are clearly contributing to the final spectrum. This is proven by inspection of the region above 1650 cm^{-1} , where the substrate practically does not absorb. Comparison of the measured and simulated spectra clearly shows that the band at 1765 cm^{-1} should be assigned to **2**, while the band at 1686 cm^{-1} originates from **3**. Both bands are asymmetric, indicating the presence of both rotamers. We finally note that the excellent agreement between theory and experiment provides another strong argument for the structural assignment of the photoproducts to **2** and **3**.

Figure 5

In order to check if the singlet oxygen interaction with **1** can lead to the formation of **2** and **3** we have irradiated the acetonitrile solution containing both **1** and **PdOEP** with green light ($\lambda_{\text{max}} = 543 \text{ nm}$). Our substrate (**1**) does not absorb at this wavelength; only the porphyrin molecules are photoexcited and they produce singlet oxygen under atmospheric conditions.⁴⁵ The electronic absorption spectra obtained before and under irradiation are presented in Figure S4 in Supporting Information. In the spectrum of the mixture of **1** and **PdOEP** the absorbance of **1** is diminished under irradiation, indicating that **1** reacts with singlet oxygen. The results of LC-MS studies (Figure S5) evidence that the protonated ion with the $m/z = 278$, assigned to compound **3**, is clearly formed, whereas the amount of the ion corresponding to the molecule **2** with the mass of 276 is much lower, about 10% of that of **3**.

Summary and Conclusions

We have shown that the 365 nm irradiation of acetonitrile solution of a 2-substituted indole derivative, 2-(1'*H*-indol-2'-yl)-[1,5]naphthyridine, in acetonitrile in the presence of air provides an easy way to obtain a benzoxazine derivative, 2-(1,5-naphthyridin-2-yl)-4H-3,1-

benzoxazin-4-one, as a major oxidation product. The second product with amide structure, N-(2-formylphenyl)-1,5-naphthyridine-2-carboxamide, according to the results of LCMS studies is formed in about four times smaller amounts than the first one. *Syn* and *anti* forms are present, both in the substrate and photoproducts.

Further work is required to elucidate the exact mechanism of UV-induced oxygenation. For now, the most plausible scenario for the production of **3** is the generation of singlet oxygen by the triplet state of the electronically excited substrate, followed by the reaction of **1** with singlet oxygen. It also explains why the photooxidation reaction does not require any additional photosensitizer, since we have used the substrate which absorbs the wavelength of radiation. The involvement of the triplet state in the photodegradation has been demonstrated earlier.³⁶

Very small amount of **2** in the experiment with external photosensitizer suggests that the formation of this species involves the reaction of excited **1** with ground state oxygen. Interestingly, the review devoted to photooxygenation of heterocycles⁴⁶ mentions the oxidative 2,3-bond cleavage, i.e., the route leading to **3**, but not the path leading to the dominant photoproduct **2**.

It can be instructive to compare our results with other, published reports for compounds containing both pyrrole and pyridine moieties, for which in-depth photochemical studies are known. These include photochemical studies of indomethacin,⁴⁷ tadalafil⁴⁸ and etodolac.⁴⁹ Somewhat surprisingly, in some of these studies^{47,48} the photochemical reaction does not take place on the pyrrole moiety, but involves the neighboring aromatic ring. Our system is more similar to etodolac,⁴⁹ a compound which, upon irradiation, becomes oxidized, forming an expanded pyrrole ring and the amide bond.

The results of this study can help in developing an efficient and easy method of synthesis of molecules with benzoxazinone structure. We plan to carry out further studies in this direction using a large library of indole-base compounds available in our laboratories.⁵⁰⁻⁵²

Conflicts of interest

There are no conflicts of interest to declare.

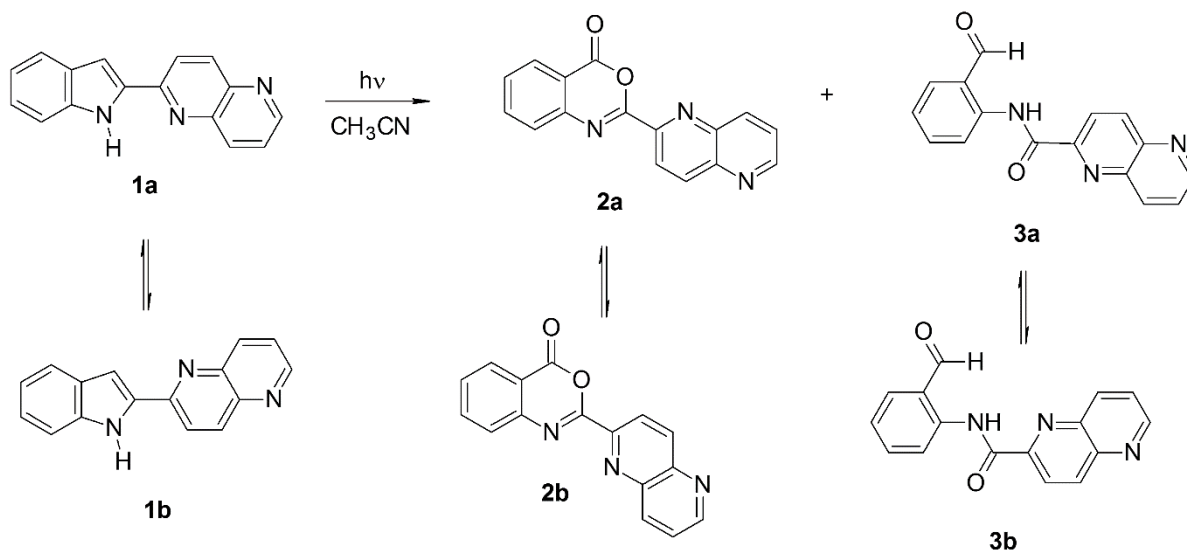
Acknowledgements

The work has been financed by the Polish National Science Centre Grant No. 2016/22/A/ST4/00029. The computations were conducted with the support of PL-Grid Infrastructure. The authors thank the Ecotoxicological Monitoring Station UKSW for providing access to the Shimadzu Nexara X2 LC/MS/MS 8050 system. R. T. thanks the U.S. Department of Energy, Office of Science, Office of Basic Energy Sciences under award no. DE-FG02-07ER15888 and the Robert A. Welch Foundation (E-621).

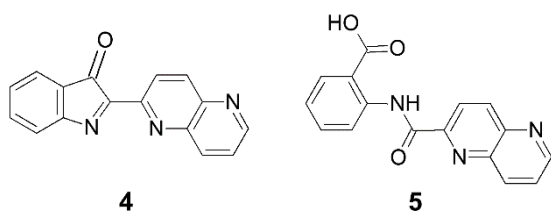
References

- 1 S. Prasad Kunapuli, N. Ullah Kern and C. S. Vaidyanathan, *J. Indian Inst. Sci*, 1981, **63**, 167–202.
- 2 M. Mentel and R. Breinbauer, *Curr. Org. Chem.*, 2007, **11**, 159–176.
- 3 D. Creed, *Photochem. Photobiol.*, 1984, **39**, 537–562.
- 4 E. Silva, *Biol. Res.*, 1996, **29**, 57–67.
- 5 B. A. Kerwin and R. L. Remmele, *J. Pharm. Sci.*, 2007, **96**, 1468–1479.
- 6 F. Liu, Y. Fang, Y. Chen and J. Liu, *J. Phys. Chem. B*, 2011, **115**, 9898–9909.
- 7 X.-L. Lian, H. Lei, X.-J. Quan, Z.-H. Ren, Y.-Y. Wang and Z.-H. Guan, *Chem. Commun.*, 2013, **49**, 8196–8198.
- 8 M. Yamashita and A. Iida, *Tetrahedron Lett.*, 2014, **55**, 2991–2993.
- 9 X. Jiang, C. Zheng, L. Lei, K. Lin and C. Yu, *European J. Org. Chem.*, 2018, **2018**, 1437–1442.
- 10 A. El-Mekabaty, *Int. J. Mod. Org. Chem.*, 2013, **2**, 81–121.
- 11 B. Ensley, B. Ratzkin, T. Osslund, M. Simon, L. Wackett and D. Gibson, *Science*, 1983, **222**, 167–169.
- 12 D. Murdock, B. D. Ensley, C. Serdar and M. Thalen, *Nat Biotech*, 1993, **11**, 381–386.
- 13 G. H. Han, H. J. Shin and S. W. Kim, *Enzyme Microb. Technol.*, 2008, **42**, 617–623.
- 14 E. M. J. Gillam, L. M. Notley, H. Cai, J. J. De Voss and F. P. Guengerich, *Biochemistry*, 2000, **39**, 13817–13824.
- 15 Z. L. Wu, L. M. Podust and F. P. Guengerich, *J. Biol. Chem.*, 2005, **280**, 41090–41100.
- 16 S. Hu, J. Huang, L. Mei, Q. Yu, S. Yao and Z. Jin, *J. Mol. Catal. B Enzym.*, 2010, **67**, 29–35.
- 17 K. Muniyappan, G. Chandramohan, J. Stephen and A. Periyasami, *Res. J. Chem. Sci.*, 2014, **4**, 7–11.
- 18 Y. Zi, Z. J. Cai, S. Y. Wang and S. J. Ji, *Org. Lett.*, 2014, **16**, 3094–3097.
- 19 M. S. Petrônio and V. F. Ximenes, *Luminescence*, 2013, **28**, 853–859.
- 20 A. H. Thomas, M. P. Serrano, V. Rahal, P. Vicendo, C. Claparols, E. Oliveros and C. Lorente, *Free Radic. Biol. Med.*, 2013, **63**, 467–475.
- 21 L. O. Reid, E. A. Roman, A. H. Thomas and M. L. Dántola, *Biochemistry*, 2016, **55**, 4777–4786.
- 22 N. Horlacher and W. Schwack, *Photochem. Photobiol.*, 2014, **90**, 1257–1263.
- 23 K. Huvaere and L. H. Skibsted, *J. Am. Chem. Soc.*, 2009, **131**, 8049–8060.
- 24 J. A. Silvester, G. S. Timmins and M. J. Davies, *Free Radic. Biol. Med.*, 1998, **24**, 754–766.
- 25 H. S. Garg and D. S. Bhakuni, *Indian J. Chem. Sect. B*, 1986, **25**, 973.
- 26 J. C. Powers, J. L. Asgian, Ö. D. Ekici and K. E. James, *Chem. Rev.*, 2002, **102**, 4639–4750.
- 27 U. Neumann, N. M. Schechter and M. Gütschow, *Bioorganic Med. Chem.*, 2001, **9**, 947–954.
- 28 R. L. Stein, A. M. Strimpler, B. R. Viscarello, R. A. Wildonger, R. C. Mauger and D. A. Trainor, *Biochemistry*, 1987, **26**, 4126–4130.
- 29 A. Krantz, R. W. Spencer, T. F. Tam, T. J. Liak, L. J. Copp, E. M. Thomas and S. P. Rafferty, *J. Med. Chem.*, 1990, **33**, 464–479.
- 30 P. W. Hsieh, H. P. Yu, Y. J. Chang and T. L. Hwang, *Eur. J. Med. Chem.*, 2010, **45**, 3111–3115.
- 31 P. W. Hsieh, F. R. Chang, C. H. Chang, P. W. Cheng, L. C. Chiang, F. L. Zeng, K. H. Lin and Y. C. Wu, *Bioorganic Med. Chem. Lett.*, 2004, **14**, 4751–4754.
- 32 A. M. F. Eissa and R. El-Sayed, *J. Heterocycl. Chem.*, 2006, **43**, 1161–1168.

- 33 R. L. Jarvest, M. J. Parratt, C. M. Debouck, J. G. Gorniak, L. J. Jennings, H. T. Serafinowska and J. E. Strickler, *Bioorganic Med. Chem. Lett.*, 1996, **6**, 2463–2466.
- 34 A. Macchiarulo, G. Costantino, D. Fringuelli, A. Vecchiarelli, F. Schiaffella and R. Fringuelli, *Bioorganic Med. Chem.*, 2002, **10**, 3415–3423.
- 35 O. M. O. Habib and H. M. Hassan, Ahmed El-Meka, *Am. J. Org. Chem.*, 2012, **2**, 45–51.
- 36 B. Golec, M. Kijak, V. Vetokhina, A. Gorski, R. P. Thummel, J. Herbich and J. Waluk, *J. Phys. Chem. B*, 2015, **119**, 7283–7293.
- 37 B. Golec, K. Nawara, A. Gorski, R. P. Thummel, J. Herbich and J. Waluk, *Phys. Chem. Chem. Phys.*, 2018, **20**, 13306–13315.
- 38 U. Mazzucato and F. Momicchioli, *Chem. Rev.*, 1991, **91**, 1679–1719.
- 39 C. H. Yoder, S. Kennedy and F. A. Snavely, 1978, **43**, 1077–1079.
- 40 S. Jolivet, F. Texier-Boullet, J. Hamelin and P. Jacquault, *Heteroat. Chem.*, 1995, **6**, 469–474.
- 41 S. A. Syrbu, T. V Lyubimova and A. S. Semeikin, *Chem. pf Heterocycl. Compd.*, 2004, **40**, 1464–1472.
- 42 C. Lee, W. Yang and R. G. Parr, *Phys. Rev. B*, 1988, **37**, 785–789.
- 43 A. D. Becke, *Phys. Rev. A*, 1988, **38**, 3098–3100.
- 44 M. J. Frisch, G. W. Trucks, H. B. Schlegel, G. E. Scuseria, M. A. Robb, J. R. Cheeseman, G. Scalmani, V. Barone, B. Mennucci, G. A. Petersson, H. Nakatsuji, M. Caricato, X. Li, H. P. Hratchian, A. F. Izmaylov, J. Bloino, G. Zheng, J. L. Sonnenberg, M. Hada, M. Ehara, K. Toyota, R. Fukuda, J. Hasegawa, M. Ishida, T. Nakajima, Y. Honda, O. Kitao, H. Nakai, T. Vreven, J. A. Montgomery, J. E. Peralta, F. Ogliaro, M. Bearpark, J. J. Heyd, E. Brothers, K. N. Kudin, V. N. Staroverov, R. Kobayashi, J. Normand, K. Raghavachari, A. Rendell, J. C. Burant, S. S. Iyengar, J. Tomasi, M. Cossi, N. Rega, J. M. Millam, M. Klene, J. E. Knox, J. B. Cross, V. Bakken, C. Adamo, J. Jaramillo, R. Gomperts, R. E. Stratmann, O. Yazyev, A. J. Austin, R. Cammi, C. Pomelli, J. W. Ochterski, R. L. Martin, K. Morokuma, V. G. Zakrzewski, G. A. Voth, P. Salvador, J. J. Dannenberg, S. Dapprich, A. D. Daniels, Farkas, J. B. Foresman, J. V Ortiz, J. Cioslowski and D. J. Fox, *Gaussian 09, Revis. B.01*, Gaussian, Inc., Wallingford CT, 2009.
- 45 A. Semeikin, J. Solariski, A. Gorski, E. Zenkevich, A. Starukhin, V. Knyukshto, T. Lyubimova and M. Kijak, *J. Photochem. Photobiol. A Chem.*, 2018, **354**, 101–111.
- 46 M. Iesce, F. Cermola and F. Temussi, *Curr. Org. Chem.*, 2005, **9**, 109–139.
- 47 A. Weedon and F. Wong, *J. Photochem. Photobiol A*, 1991, **61**, 27–33.
- 48 F. Temussi, G. Bassolino, F. Cermola, M. Dellagreca, M. R. Iesce, S. Montanaro, L. Previtiera and M. Rubino, *Photochem. Photobiol. Sci.*, 2010, **9**, 1139–1144.
- 49 M. Lavorgna, M. Isidori, F. Cermola, M. Brigante, E. Criscuolo, M. R. Iesce, M. DellaGreca and M. Passananti, *Sci. Total Environ.*, 2015, **518–519**, 258–265.
- 50 A. Kyrychenko, J. Herbich, F. Wu, R. P. Thummel and J. Waluk, *J. Am. Chem. Soc.*, 2000, **122**, 2818–2827.
- 51 A. Kyrychenko, J. Herbich, M. Izydorzak, F. Wu, R. P. Thummel and J. Waluk, *J. Am. Chem. Soc.*, 1999, **121**, 11179–11188.
- 52 I. Petkova, M. S. Mudadu, A. Singh, R. P. Thummel, I. H. M. Van Stokkum, W. J. Buma and J. Waluk, *J. Phys. Chem. A*, 2007, **111**, 11400–11409.



Scheme 1. The structures of the studied indole derivative, 2-(1'H-indol-2'-yl)-[1,5]naphthyridine (**1**) and of its possible oxidation products: 2-(1,5-naphthyridin-2-yl)-4H-3,1-benzoxazin-4-one (**2**) and N-(2-formylphenyl)-1,5-naphthyridine-2-carboxamide (**3**).



Scheme 2. The structures of 2-(1,5-naphthyridin-2-yl)-3H-indol-3-one (**4**) and 2-[(1,5-naphthyridine-2-carbonyl)amino]benzoic acid (**5**).

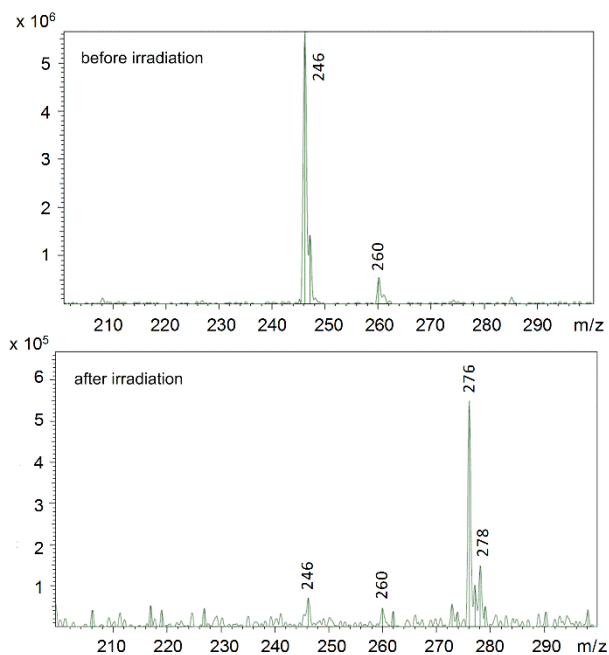


Figure 1. The ESI-MS (positive ion mode) spectra of **1** in acetonitrile before (top) and after 3 h of 365 nm irradiation (bottom).

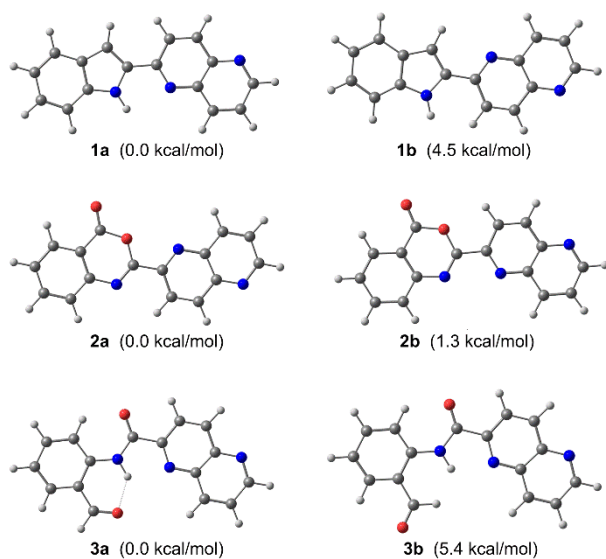


Figure 2. The predicted structures of two possible conformers of **1** and **2**, and two most stable conformers of **3** with their zero-point corrected relative energies.

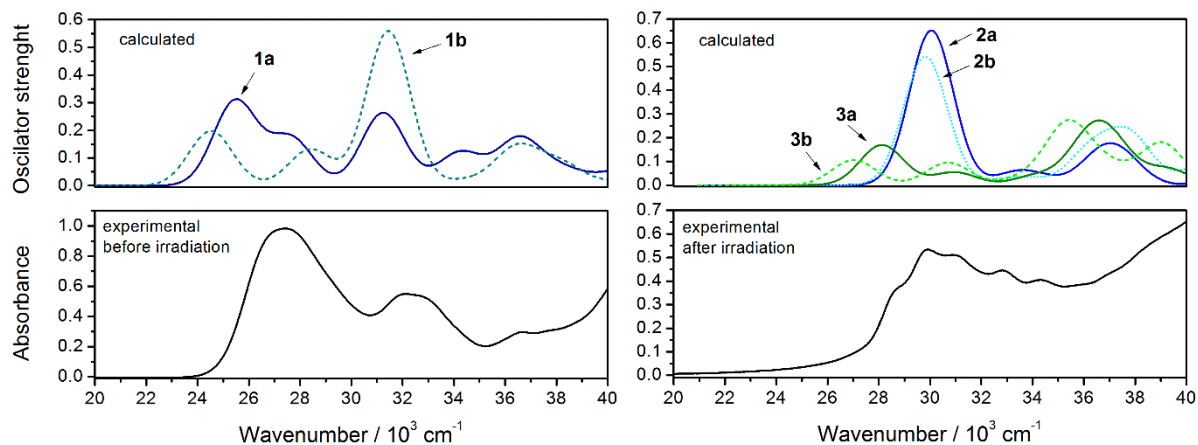


Figure 3. The comparison of the experimental absorption spectra of **1** measured before (left) and after 3 h of 365 nm irradiation (right) with the simulated spectra of two most stable rotameric forms of **1**, **2**, and **3**. The spectral envelopes were obtained by convolution of the respective stick spectra with a Gaussian function of 2000 cm⁻¹ fwhm.

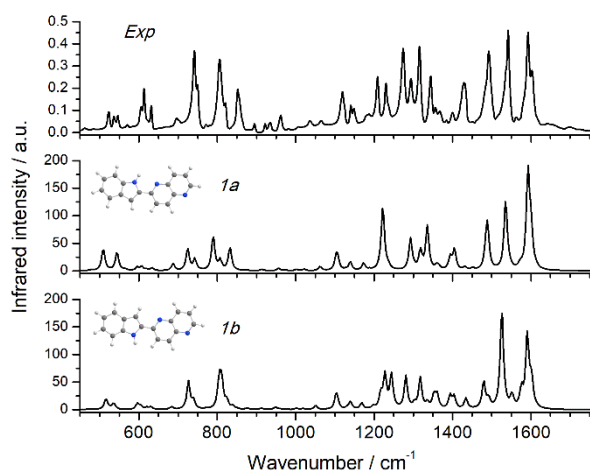


Figure 4. The comparison of the experimental and simulated infrared spectra of **1**. The calculated frequencies are scaled by the factor of 0.97.

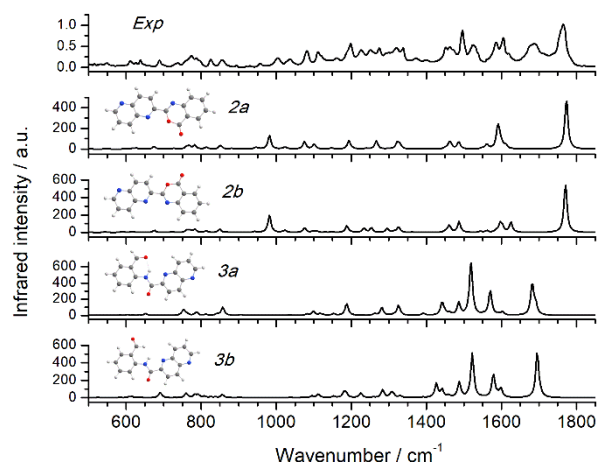
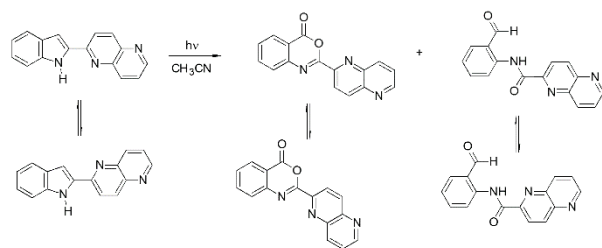


Figure 5. The comparison of the experimental infrared spectra of **1** after 6.5 h of 365 nm irradiation with the simulated spectra of two most stable conformers of **2** and **3**. The calculated frequencies are scaled by the factor of 0.97.



UV-induced photooxidation of 2-substituted indole derivative provides an efficient way to formation of benzoxazinone derivative.